NASA TECHNICAL NOTE

NASA TN D-5752

EXPERIMENTS ON THE STABILITY OF WATER-LUBRICATED THREE-SECTOR HYDRODYNAMIC JOURNAL BEARINGS AT ZERO LOAD

by Fredrick T. Schuller and William J. Anderson

Lewis Research Center
Cleveland, Ohio

NATIONAL AERONAUTICS AND SPACE ADMINISTRATION • WASHINGTON, D. C. • APRIL 1970

1. Report No. NASA TN D-5752	2. Government Accession No.	3. Recipient's Catalog No.
4. Title and Subtitle EXPERIMENTS ON THE STABILITY OF WATER-LUBRICATED THREE-SECTOR HYDRODYNAMIC JOURNAL BEARINGS AT ZERO LOAD		5. Report Date April 1970 6. Performing Organization Code
7. Author(s) Fredrick T. Schuller and William J. Anderson		8. Performing Organization Report No. E-5434
9. Performing Organization Name and Address Lewis Research Center, National Aeronautics and Space Administration, Cleveland, Ohio 44135		10. Work Unit No. 129-03 11. Contract or Grant No. 13. Type of Report and Period Covered Technical Note
12. Sponsoring Agency Name and Address National Aeronautics and Space Administration, Washington, D.C. 20546		14. Sponsoring Agency Code

15. Supplementary Notes

16. Abstract

Hydrodynamic journal bearing stability tests were conducted with three-sector bearings. The bearings, consisting of three 115° sectors with a nominal 1.5-in. (3.8-cm) diameter, were tested in water at 80° F (300 K) at speeds to 9000 rpm with zero load. Three-sector bearings with a wholly-converging-film geometry were more stable than those with a converging-diverging film geometry. Three-sector bearings with wholly-converging-film-geometry were generally more stable and less sensitive to clearance than herringbone-grooved bearings.

17. Key Words (Suggested by Author(s))
Water bearing tests
Hydrodynamic bearings
Bearing stability
Three-sector bearings

18. Distribution Statement
Unclassified - unlimited

19. Security Classif. (of this report)	20. Security Classif. (of this page)	21. No. of Pages	22. Price*
Unclassified	Unclassified	21	$3.00

*For sale by the Clearinghouse for Federal Scientific and Technical Information
Springfield, Virginia 22151

EXPERIMENTS ON THE STABILITY OF WATER-LUBRICATED THREE-SECTOR HYDRODYNAMIC JOURNAL BEARINGS AT ZERO LOAD

by Fredrick T. Schuller and William J. Anderson

Lewis Research Center

SUMMARY

A series of stability tests was conducted with 1.5-inch- (3.8-cm-) diameter, 1.5-inch- (3.8-cm-) long, three-sector hydrodynamic journal bearings in water at 80° F (300 K) at speeds to 9000 rpm with zero load. The bearings consisted of three 115° sectors. Two types of three-sector bearings were run: one had a converging-diverging-film geometry and the other had a wholly-converging geometry. Three-sector bearings with a wholly-converging-film geometry were more stable than those with converging-diverging geometry. Three-sector bearings with a wholly-converging-film geometry were generally more stable and less sensitive to clearance than herringbone-grooved bearings. Dimensionless speed Γ was a more desirable parameter to use with dimensionless mass $\overline{M}$ than was the preload coefficient δ when determing the stability characteristics of three-sector bearings that are not centrally lobed.

INTRODUCTION

The ability of a journal bearing to inhibit self-excited fractional-frequency whirl is of prime importance for successful operation of a power generation system for space vehicles. In this type of whirl, the journal center tends to orbit the bearing center at an angular velocity about one-half that of the journal around its own center (ref. 1). Rankine cycle space power systems must function in a zero-gravity environment at high shaft speeds and with low-viscosity lubricants (alkali metals). All these factors tend to produce the instability that must be inhibited. Since the environment cannot be altered, the problem must be solved by selecting bearing configurations that are least likely to exhibit whirl under these environmental conditions.

Tilting pad bearings are exceptionally stable but are complex since they are composed of several parts and are subject to pivot surface damage (ref. 1). A more prac-

tical bearing would be one with a fixed geometry. One such bearing that showed good stability properties is the herringbone-grooved bearing (refs. 2 to 4). Another fixed-geometry bearing that has shown promise is the lobed bearing (ref. 5), which has a marked similarity to the tilting pad bearing except that its pads (lobes) are fixed in one position. Most of the research on lobed bearings has been done with bearings that are centrally lobed, which results in a converging-diverging-film generation as the shaft rotates within them. In a centrally lobed bearing, only the converging wedge portion of the arc of each lobe is active in generating load capacity. If the lobe is tilted toward its trailing edge, the minimum film thickness approaches the trailing edge of the lobe, and a pressure profile is built up over a larger portion of the lobe arc, which increases its load capacity (ref. 6). Reference 6 reports an improvement in the stability of lobed bearings with sectors tilted toward the trailing edge over those that were centrally lobed.

In the investigation reported herein, some of the bearing sectors were tilted at the trailing edge to result in a wholly-converging wedge with a minimum radial clearance at the trailing edge and a maximum at the leading edge of each sector. The rest were tilted at a point 60 percent of the arc length from the leading edge of the sector, which resulted in a converging-diverging wedge approximating the geometry of a centrally lobed bearing.

The objectives of this study were (1) to compare the stability of a three-sector bearing having a converging-diverging film with that having a wholly-converging film, (2) to observe the effect of sector leading edge clearance on stability, (3) to compare the stability of three-sector bearings with that of herringbone-grooved bearings, and (4) to compare experimental stability data for three-sector bearings with analytical predictions of stability.

A three-sector bearing configuration was selected for this study mainly because this arrangement affords greater load capacity than one having more than three sectors and because theoretical data are available for three-sector bearings. The bearings had a nominal 1.5-inch (3.8-cm) diameter and were 1.5 inch (3.8 cm) long. They were submerged in water at an average temperature of 80° F (300 K) and were operated hydrodynamically at journal speeds to 9000 rpm.

SYMBOLS

a preload (ellipticity), in.; mm

C bearing radial clearance, $R_{PC} - R$, in.; mm

C_o bearing radial clearance at zero preload, $R_P - R$, in.; mm

D journal diameter, in.; cm

g gravitational constant, in./sec^2; m/sec^2

L bearing length, in.; cm

M rotor mass per bearing, W_r/g, (lb)(sec^2)/in.; (kg)(sec^2)/m

$\overline{M}$ dimensionless mass parameter, $MP_a(C/R)^5/2\mu^2L$

$\overline{M}_o$ dimensionless rotor mass parameter, $C_oMN_s/\mu DL(R/C_o)^2$ (ref. 5)

N_s journal speed, rps

N_w journal fractional-frequency-whirl onset speed at zero load, rpm

P_a atmospheric pressure, psia; N/m^2 abs

R journal radius, in.; cm

R_P radius of sector, in.; cm

R_{PC} radius of pitch circle, in.; cm

ΔR_L leading edge entrance wedge thickness, in.; mm

W_r total weight of test vessel, lb; N

α film thickness ratio, $1 + (\Delta R_L/C)$

β sector arc length, deg

Γ dimensionless speed parameter, $6\mu\omega R^2/P_aC^2$

δ preload coefficient, $a/(R_P - R)$

μ lubricant dynamic viscosity, (lb)(sec)/in.^{2}; (N)(sec)/m^2

ω journal angular speed, rad/sec

APPARATUS

Test Bearings

Three-sector bearings consisting of three 115^o sectors were mounted in a solid housing by hold-down screws (figs. 1 and 2) and were evaluated. Each sector of one particular bearing assembly was ground to its specified contour while it was the only sector assembled in the housing. Three sectors with identical internal contours were then assembled in a common housing to form a three-sector bearing, as shown in figure 1.

Two different contours were employed in the bearing sectors to give one bearing a converging-diverging film (fig. 3(a)) in operation and another bearing a wholly-converging film (fig. 3(b)). The converging-diverging contour was designed with the minimum radial clearance at a point approximately 60 percent of the sector arc length

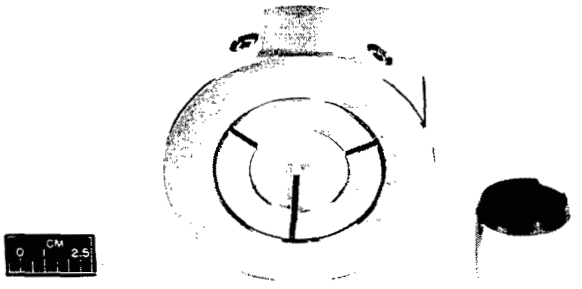

C-69-3037

Figure 1. - Three-sector lobed bearing configuration.

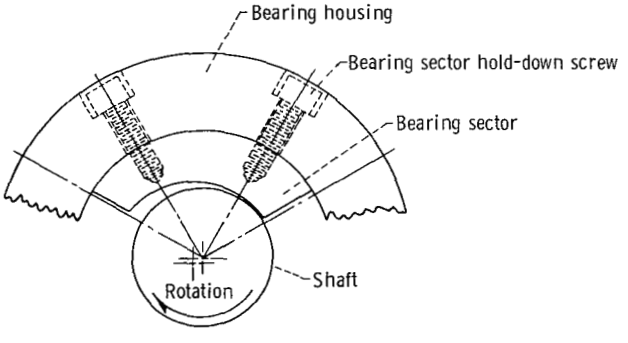

Figure 2. - Three-sector bearing assembly.

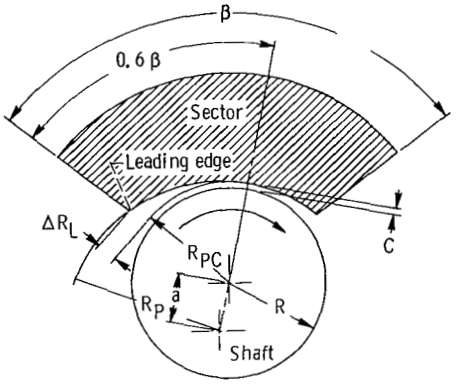

(a) Converging-diverging configuration.

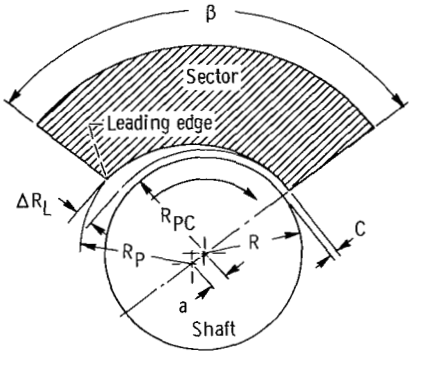

(b) Wholly-converging configuration.

Figure 3. - Sector bearing geometry.

TABLE I. - TEST RESULTS FOR THREE-SECTOR BEARINGS WITH CONVERGING-DIVERGING-FILM GEOMETRY

Bearing	Leading edge entrance wedge thickness, ΔR_L		Preload (ellipticity), a		Minimum radial clearance, $C = R_{PC} - R$		Radial clearance before preload, $C_o = R_P - R$		Preload coefficient, $\delta = a/(R_P - R)$	Fractional-frequency-whirl onset speed at zero load, N_w, rpm	Film thickness ratio, $\alpha = 1 + (\Delta R_L/C)$
	μin.	mm	μin.	mm	μin.	mm	μin.	mm			
7	500	0.013	1000	0.025	700	0.018	1700	0.043	0.59	7400	1.71
					1050	.027	2100	.053	.48	2400	1.46
					1600	.041	2600	.066	.38	510	1.31
					2100	.053	3100	.079	.32	290	1.24
9	1500	0.038	2900	0.074	600	0.015	3500	0.089	0.83	5700	3.50
					1000	.025	3900	.099	.74	1800	2.50
					1500	.038	4400	.112	.66	600	2.00
					2150	.055	5100	.130	.57	460	1.70
10	2800	0.071	4600	0.117	600	0.015	5200	0.132	0.89	5800	5.67
					1050	.027	5600	.142	.82	2200	3.67
					1550	.039	6100	.155	.75	1200	2.80
					2100	.053	6600	.168	.70	800	2.33
11	4200	0.107	7800	0.198	800	0.020	8600	0.218	0.91	5200	6.30
					1200	.030	9000	.228	.87	1200	4.50
					1700	.043	9500	.241	.82	500	3.47
					2200	.056	10 000	.254	.78	300	2.90

from the leading edge of each sector (fig. 3(a)). The wholly-converging contour had a minimum radial clearance at the trailing edge of each sector (fig. 3(b)). The various minimum radial clearances (see tables I and II) were obtained by varying the outside diameter of the journals for each bearing tested. Circumferential profile traces were made of the internal surface of each sector in each bearing assembly in three planes along the length of the bearing to obtain the leading edge entrance wedge thicknesses ΔR_L (fig. 3). These thicknesses are listed in tables I and II. Typical surface profile traces are shown in figure 4, which illustrates how the ΔR_L values were obtained.

The assembled bearings in all cases had a nominal 1.5-inch (3.8-cm) length and diameter. The inside surfaces of the bearing sectors and journal outside diameter were machined to a 4- to 8-microinch (0.1- to 0.2-μm) rms finish. The journals were made of stainless steel and the bearing sectors of bronze.

TABLE II. - TEST RESULTS FOR THREE-SECTOR BEARINGS WITH

WHOLLY-CONVERGING-FILM GEOMETRY

Bearing	Leading edge entrance wedge thickness, ΔR_L		Preload (ellipticity), a		Minimum radial clearance, $C = R_{PC} - R$		Radial clearance before preload, $C_o = R_P - R$		Preload coefficient, $\delta = a/(R_P - R)$	Fractional-frequency-whirl onset speed at zero load, N_w, rpm	Film thickness ratio, $\alpha = 1 + (\Delta R_L/C)$
	μin.	mm	μin.	mm	μin.	mm	μin.	mm			
8	600	0.015	500	0.013	850	0.022	1350	0.034	0.37	4600	1.71
					1200	.030	1700	.043	.29	1900	1.50
					1750	.044	2250	.057	.22	500	1.34
					2250	.057	2750	.070	.18	200	1.27
6	1400	0.036	1100	0.028	650	0.017	1800	0.046	0.61	9000	3.15
					950	.024	2000	.051	.55	6500	2.47
					1350	.034	2400	.061	.46	5000	2.04
					1950	.050	3000	.076	.37	1700	1.72
3	2600	0.066	2100	0.053	600	0.015	2700	0.069	0.78	7400	5.33
					1000	.025	3100	.079	.68	6500	3.60
					1500	.038	3600	.091	.58	4800	2.73
					2050	.052	4200	.107	.50	4000	2.27
1	3900	0.099	3100	0.079	600	0.015	3700	0.094	0.84	4900	7.50
					950	.024	4000	.102	.77	5000	5.10
					1450	.037	4600	.117	.67	3000	3.69
					1950	.050	5100	.130	.61	1900	3.00

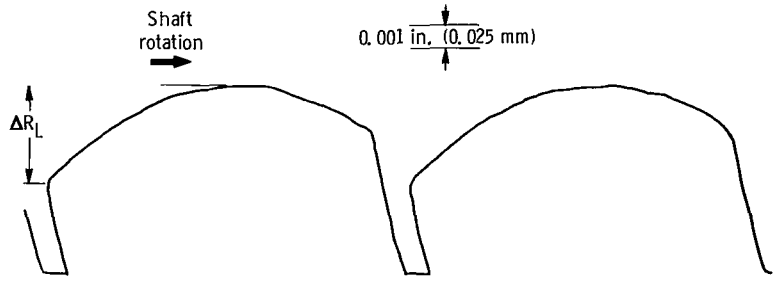

(a) Converging-diverging configuration.

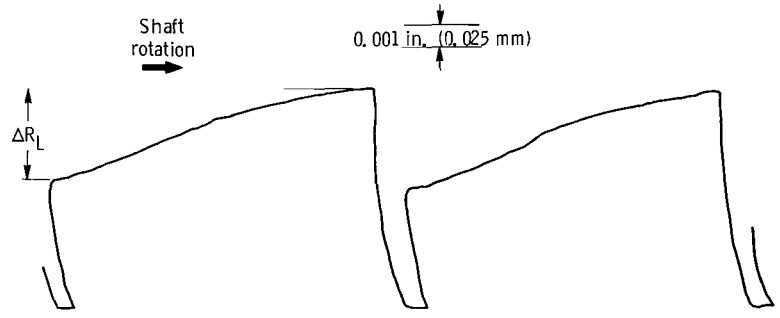

(b) Wholly-converging configuration.

Figure 4. - Typical circumferential profile trace of inside surface of bearing sectors.

Bearing Test Apparatus

The test vessel and associated parts are shown in figure 5. The shaft is positioned vertically so that gravity forces do not load the bearing. The test vessel, which also serves as the test bearing housing, floats between the upper and lower gas bearings. Bearing torque can be measured, if desired, by a force transducer attached to the floating test vessel.

Movement of the test vessel during a test is measured by orthogonally mounted capacitance probes outside the test vessel. The output of the probes is connected to an X, Y-display on an oscilloscope where this motion can be observed. The orbital frequency of the test vessel motion was measured by a frequency counter. A more detailed description of the test apparatus and instrumentation is given in reference 2.

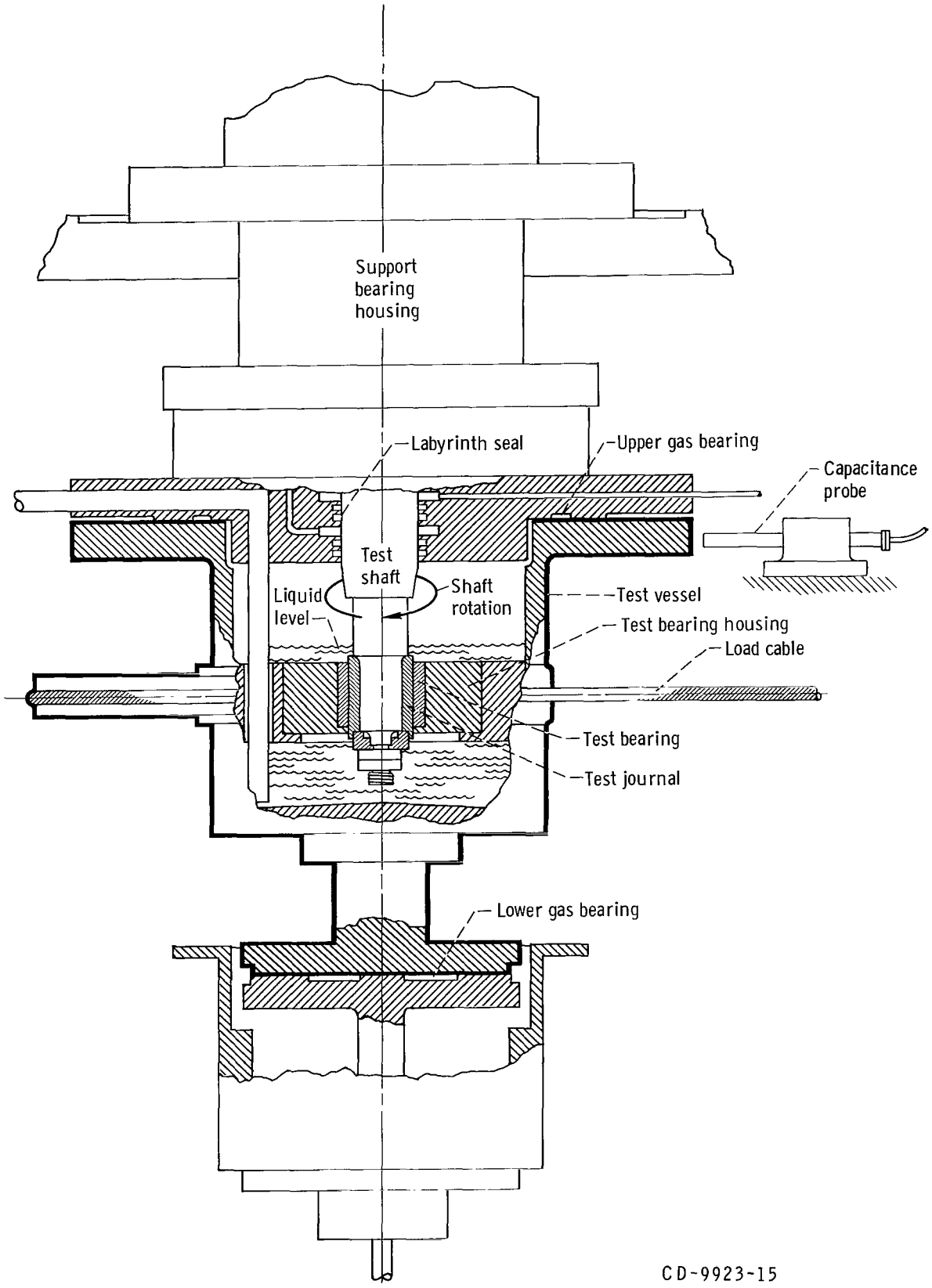

Figure 5. - Bearing test apparatus.

PROCEDURE

Details of the test procedure are given in reference 2. The bearings were run at zero load throughout the entire test. The onset of whirl was noted by observing the bearing housing motion on the oscilloscope screen (ref. 2), and the shaft speed was recorded at this time. Damage to the test bearings due to fractional-frequency whirl was prevented by reducing the speed immediately after photographing the whirl pattern on the oscilloscope screen.

In these experiments, the motion of the bearing with its massive housing was monitored. Thus, the journal axis was fixed while the bearing axis whirled. The validity of the stability data obtained in this manner was established in reference 2, where excellent correlation was obtained between theoretical and experimental data for a three-axial-grooved bearing run in water with a plain journal.

RESULTS AND DISCUSSION

General

In these experiments, the leading edge entrance wedge thickness ΔR_L (figs. 3 and 4) was used as a parameter for comparing the stability characteristics of converging-diverging bearings with wholly-converging-film three-sector bearings. Both types of bearings were run at four different radial clearances C for each of four values of ΔR_L.

The preload coefficient δ of a converging-diverging-film bearing is different from that of a wholly-converging-film bearing, assuming that both have the same ΔR_L and clearance, as shown in figure 6. For example, at a ΔR_L value of 3000 microinches (0.076 mm), the preload coefficient for a converging-diverging-film bearing at a radial clearance C of 2100 microinches (0.053 mm) is 0.71, while for a wholly-converging-film bearing it is only 0.54. In this report, therefore, preload coefficient is only used when experimental data are compared with referenced theoretical data for which the preload coefficient was used as one of the parameters.

The results of 32 stability tests that covered a range of ΔR_L values from 500 to 4200 microinches (0.013 to 0.107 mm) are shown in tables I and II and in figures 7 to 13.

Effect of Bearing Configuration on Stability

The experimental results obtained with three-sector bearings having a converging-diverging-film and a wholly-converging-film geometry are shown in figure 7. In the

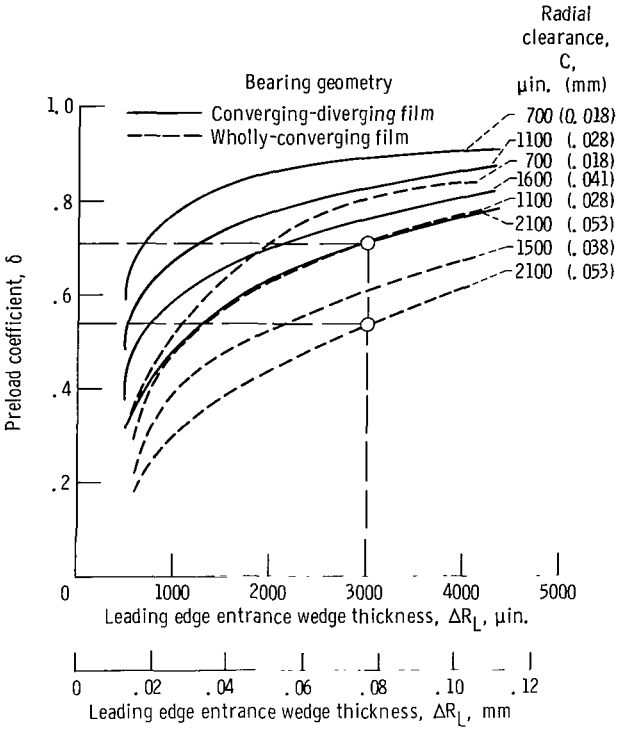

Figure 6. - Preload coefficient as function of leading edge entrance wedge thickness at various radial clearances for two different bearing sector configurations.

area labeled stable operation, to the left of the experimental curves, the bearings ran stably at zero load; immediately to the right of the curves, fractional-frequency whirl occurred. The experimental curves represent the stability limits of the bearings tested and indicate the zero-load threshold of stability. The dimensionless rotor mass and speed parameters $\overline{M}$ and Γ, respectively, were obtained from the theoretical stability analysis of reference 2. The average leading edge entrance wedge thickness ΔR_L for the converging-diverging-film and wholly-converging-film bearings (the stability curves for which are depicted in fig. 7(a)) was 550 microinches (0.014 mm). At this value of ΔR_L, the bearings of the two different film geometries had essentially the same stability characteristics.

A study of figure 7 shows that the wholly-converging-film bearing is more stable for all ΔR_L values ranging from 1450 to 4050 microinches (0.037 to 0.103 mm), with one possible exception. In figure 7(d), at a ΔR_L value of 4050 microinches (0.103 mm) and an $\overline{M}$ value of 0.11, the curve representing the converging-diverging-film bearing tends to cross over that of the wholly-converging-film bearing, which indicates that a converging-diverging-film bearing might be more stable at $\overline{M}$ values below 0.11 at a ΔR_L of 4050 microinches (0.103 mm).

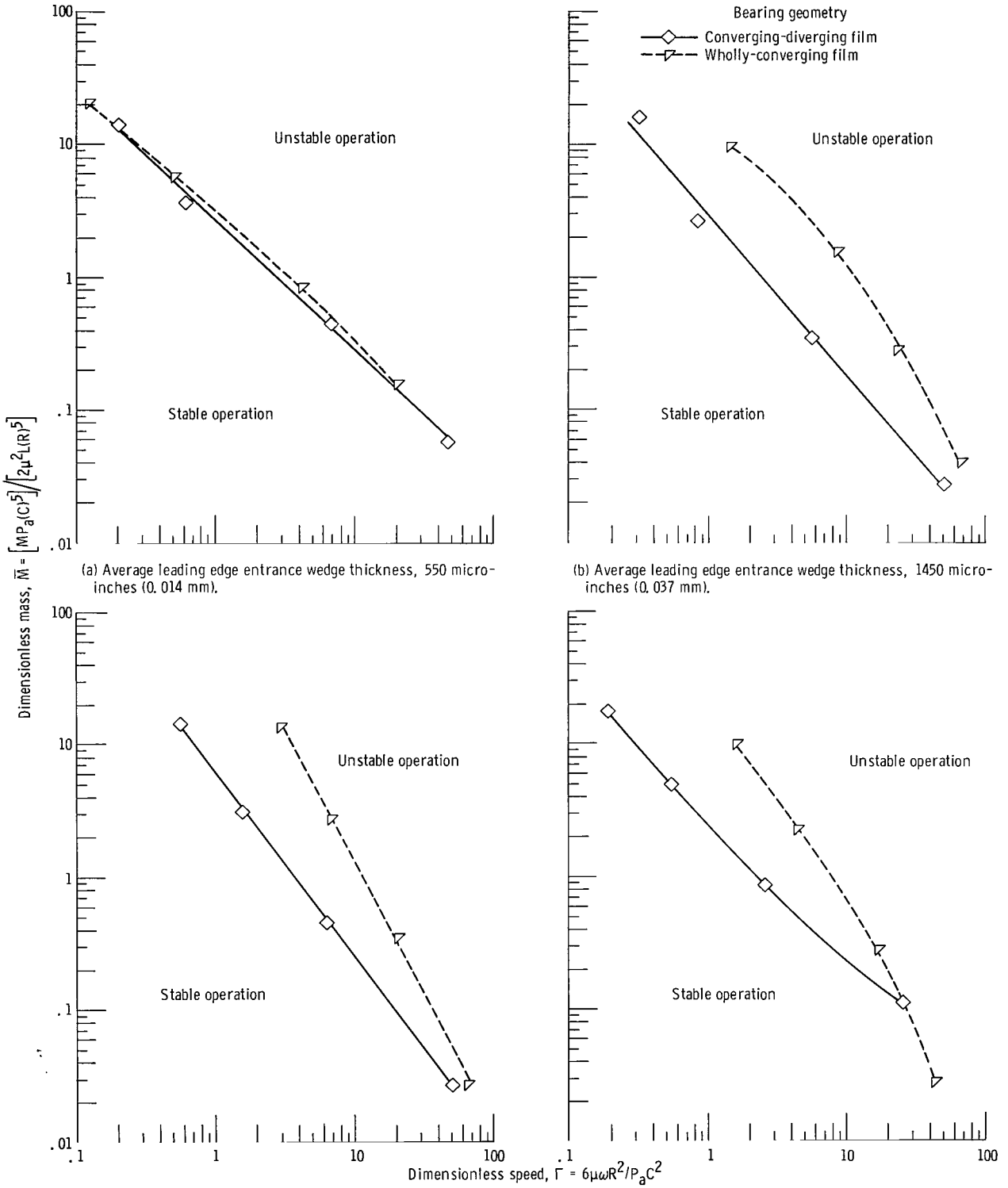

(a) Average leading edge entrance wedge thickness, 550 micro-inches (0. 014 mm).

(b) Average leading edge entrance wedge thickness, 1450 micro-inches (0. 037 mm).

(c) Average leading edge entrance wedge thickness, 2700 micro-inches (0. 014 mm).

(d) Average leading edge entrance wedge thickness, 4050 micro-inches (0. 103 mm).

Figure 7. - Effect of bearing configuration on stability of three-sector bearings at various leading edge entrance wedge thicknesses.

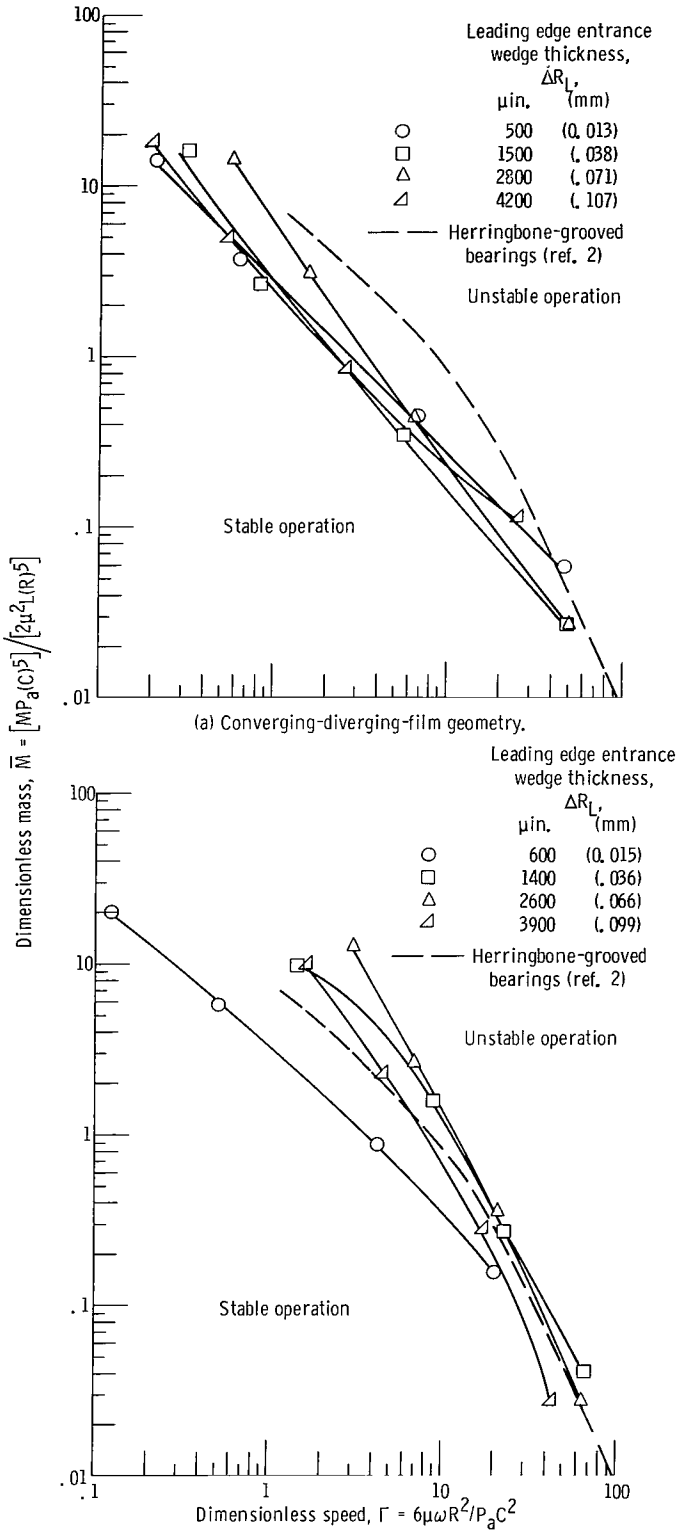

(a) Converging-diverging-film geometry.

(b) Wholly-converging-film geometry.

Figure 8. - Effect of leading edge entrance wedge thickness on stability of three-sector bearing.

With a converging-diverging-film shape, only a portion of the arc of each lobe (the converging wedge portion) is active in generating load capacity. Increased load capacity and stability can be attained by using more of the arc of each lobe to build up pressure (ref. 6). This is accomplished by tilting the bearing sector on its trailing edge.

Effect of Leading Edge Entrance Wedge Thickness on Stability

Figures 8(a) and (b) show the effect of leading edge entrance wedge thickness ΔR_L on the stability of converging-diverging-film and wholly-converging-film bearings, respectively. A maximum in stability exists at a ΔR_L of 2800 microinches (0.071 mm) for values of $\overline{M}$ above 0.44 for the converging-diverging-film bearings (fig. 8(a)). Below this value, the bearings with a ΔR_L value of 500 and 4200 microinches (0.013 and 0.107 mm) were the most stable.

An optimum in stability for the wholly-converging-film bearings existed at a ΔR_L value of 2600 microinches (0.066 mm) (fig. 8(b)) for values of $\overline{M}$ above 0.35, with very little reduction in stability at lower $\overline{M}$ values. It is interesting to note that optimum stability for both the converging-diverging-film and the wholly-converging-film bearings occurred at almost the same ΔR_L values, namely, 2800 and 2600 microinches (0.071 and 0.066 mm), respectively, for higher values of $\overline{M}$. Also, there was a considerable gain in stability with the wholly-converging-film bearings when the ΔR_L value of 600 microinches (0.015 mm) increased (fig. 8(b)).

Comparison of Theoretical and Experimental Stability Data for Three-Sector Bearings

The solid curves shown in figure 9 are from reference 5 and show the theoretical stability threshold of three-lobed bearings that are centrally lobed. Since the Reynolds number of the experimental points reported herein fell within the range of 0 to 2000, both curves have been included. The experimental data were plotted using the parameters of reference 5 and show fair agreement with the theoretical values for the converging-diverging-film bearing, as shown in figure 9(a). Some of the deviation in the experimental data from the theoretical curves might result from the fact that the theoretical curves are based on a centrally lobed configuration whereas the experimental data were obtained from a noncentralized lobe configuration (fig. 3(a)). This deviation is shown more strikingly in figure 9(b), where the experimental data for a wholly-converging-film-geometry bearing (fig. 3(b)) are plotted along with the identical theoretical curves in figure 9(a) for a centrally lobed bearing configuration. Much of the experimental data shows a more stable bearing than theory predicts. The scatter of

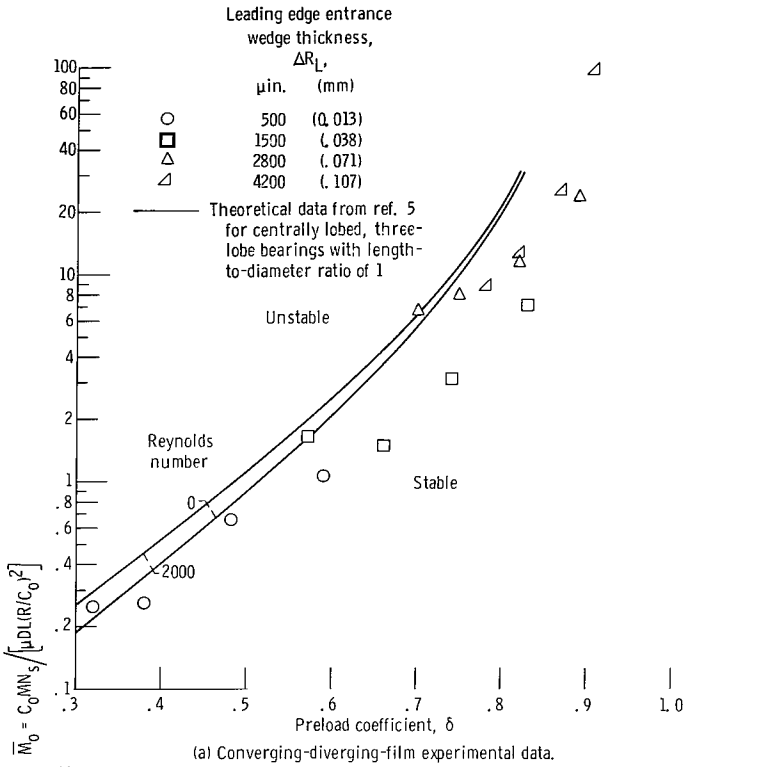

(a) Converging-diverging-film experimental data.

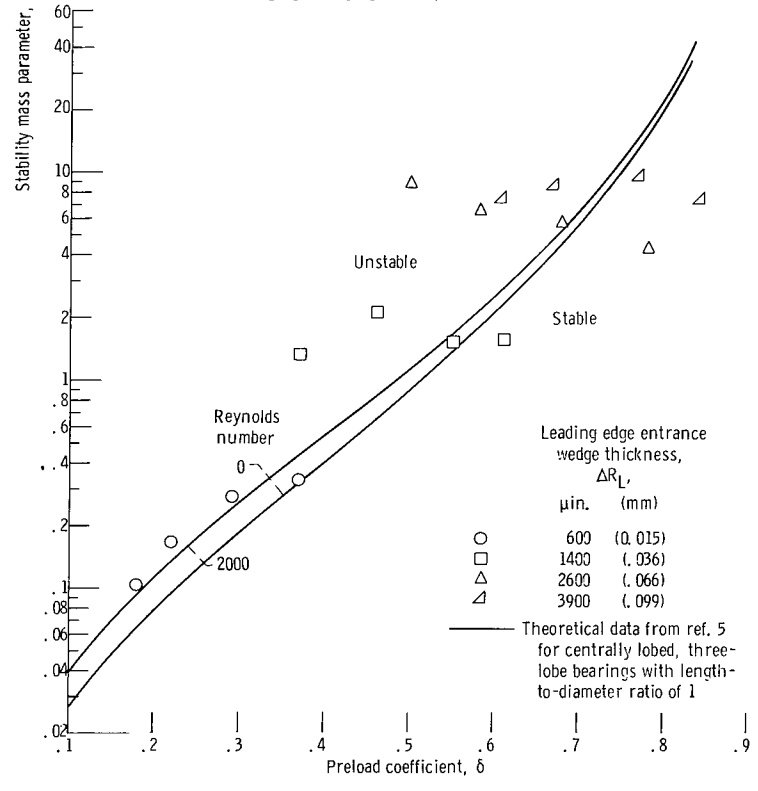

(b) Wholly-converging-film experimental data.

Figure 9. - Comparison of theoretical and experimental data using dimensionless parameters of reference 5.

experimental data is more pronounced with the wholly-converging film because the preload coefficient δ is not the most desirable parameter to use for a three-sector bearing that is not centrally lobed. The bearing parameters $\overline{M}$ and Γ used in the previous figures give a much better measurement of bearing stability and are not dependent on the manner in which the bearing is tilted.

Stability Comparison of Three-Sector Bearings With Herringbone-Grooved Bearings

The dashed curves in figure 8 represent the mean stability of a group of herringbone-grooved bearings described in reference 2. A comparison of the stability threshold of three-sector and herringbone-grooved bearings can be made in these figures, since the same bearing parameters are used in plotting the experimental data in both cases. Figure 8(a) shows that a three-sector bearing with a converging-diverging film was generally less stable than a herringbone-grooved bearing. However, a three-sector bearing with a wholly-converging film and a ΔR_L of 1400 or 2600 microinches (0.036 or 0.066 mm) (fig. 8(b)) exhibited greater stability than the herringbone-grooved bearing, especially at the higher $\overline{M}$ values (above 1.0).

Whirl speed is plotted against radial clearance in figure 10 for the wholly-convergent three-sector bearing and for a herringbone-grooved bearing. The points for the three-sector bearing correspond to the points of maximum stability (optimum locus curve) obtained from figures 11 and 12. The points for the herringbone-grooved bearing were obtained in a similar manner from data in reference 7. Figure 10 shows that the stability of the wholly-convergent three-sector bearing is less sensitive to clearance than that of the herringbone-grooved bearing. The threshold of stability of the wholly-convergent three-sector bearing diminishes at a constant rate and to a lesser degree than that of the herringbone-grooved bearing as the radial clearance is increased above 810 microinches (0.020 mm).

Design Curves

The data were replotted in slightly different form in order to facilitate the design of optimum-geometry bearings.

Whirl onset speed is plotted against radial clearance in figure 11 for the four different values of ΔR_L for the wholly-convergent-film bearings. The values of the film thickness ratio $\alpha = 1 + (\Delta R_L/C)$ (table II) are given for each data point and represent the ratio of inlet to exit film thickness in each sector. The vertical dashed lines intersect the experimental curves at four arbitrary clearance values. The curves in figure 12

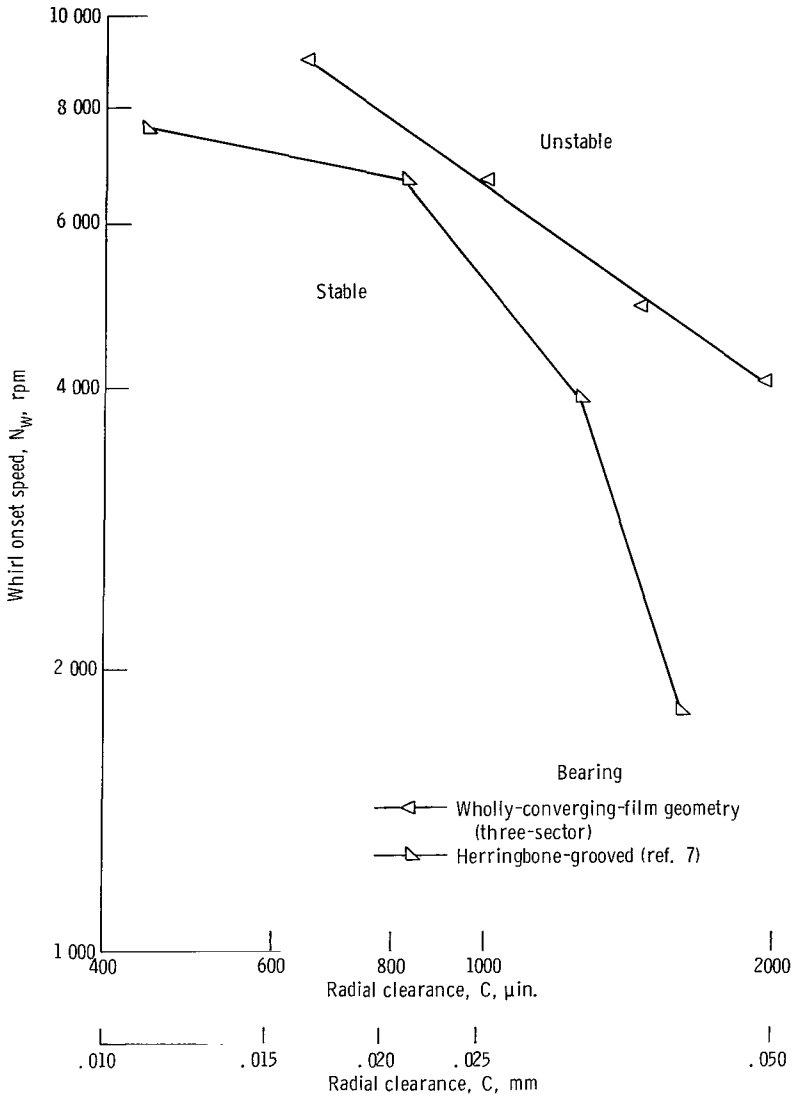

Figure 10. - Comparison of stability sensitivity with respect to clearance of three-sector wholly-converging-film-geometry bearing with that of herringbone-grooved bearing.

were obtained by cross-plotting the data in figure 11 at the four different values of clearance using the whirl speed N_W and the film thickness ratio α as the parameters. Simple straight-line interpolation was used for the cross plot. Figure 12 shows that there is an optimum value of α at any given C and that the optimum is a function of C. It also shows that stability becomes more and more sensitive to α as C increases.

Figure 13 is essentially a repetition of figure 12 except that it was plotted by using two dimensionless parameters, dimensionless speed Γ and film thickness ratio α. It is included because it is more useful as a design parameter than the curves of figure 12.

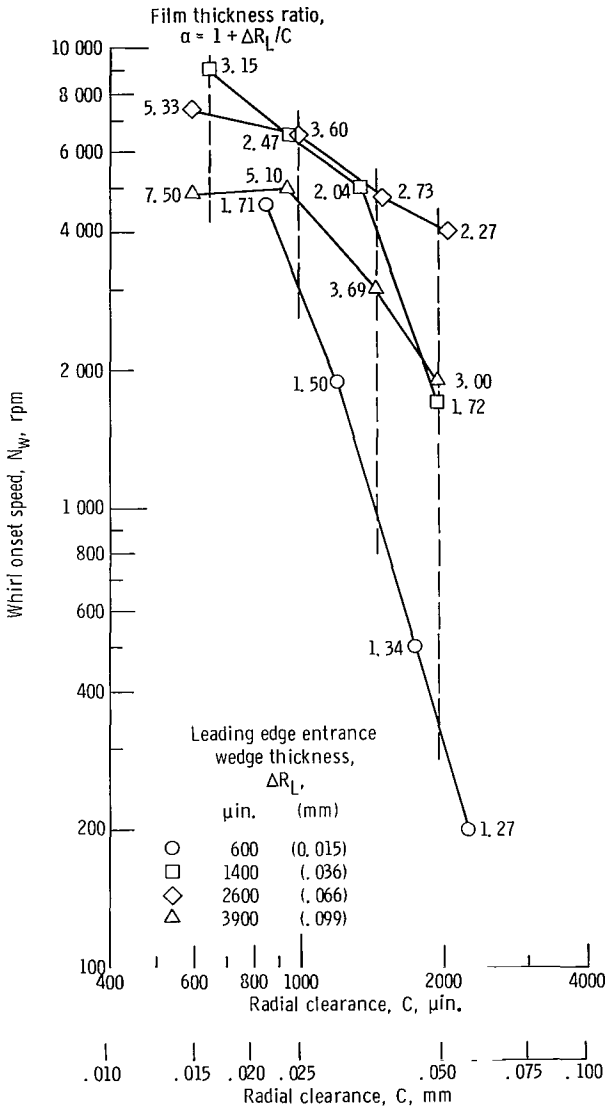

Figure 11. - Whirl onset speed as function of radial clearance for three-sector wholly-converging-film-geometry bearing at various film thickness ratios.

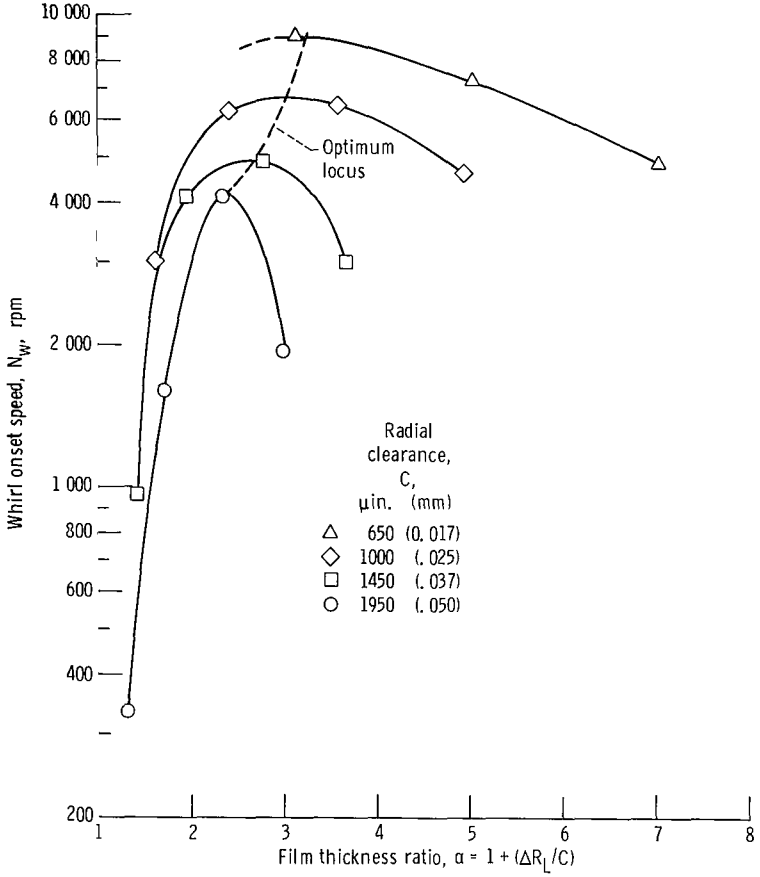

Figure 12. - Whirl onset speed as function of film thickness ratio for wholly-converging-film-geometry three-sector bearing.

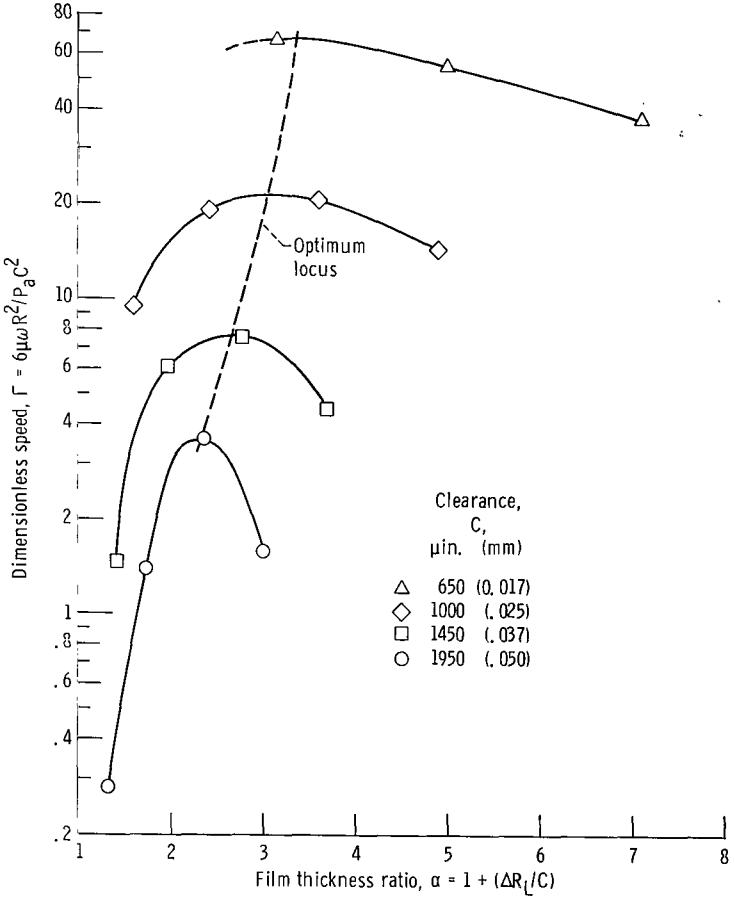

Figure 13. - Dimensionless speed as function of film thickness ratio for wholly-converging-film-geometry three-sector bearing.

SUMMARY OF RESULTS

Sixteen stability tests were performed on each of two types of three-sector bearings. One type had a converging-diverging-film geometry and the other had a wholly-converging-film geometry. Each type was run at four different radial clearances at each of four different leading edge entrance wedge thicknesses ΔR_L, which varied from 500 to 4200 microinches (0.013 to 0.107 mm). The bearings were run hydrodynamically in water at an average temperature of 80° F (300 K) at speeds to 9000 rpm. The test bearings had a nominal diameter of 1.5 inches (3.8 cm) and a length-to-diameter ratio of 1. The following results were obtained:

1. Three-sector bearings with a wholly-converging-film geometry were generally more stable than those with a converging-diverging-film geometry at similar leading edge entrance wedge thickness values.

2. An optimum-design three-sector bearing with a wholly-converging film was generally more stable than a herringbone-grooved bearing with a similar clearance, whereas the three-sector bearing with a converging-diverging film was generally less stable than a herringbone-grooved bearing.

3. The stability of a three-sector bearing with a wholly-converging-film geometry was less sensitive to radial clearance than a herringbone-grooved bearing.

4. The preload coefficient is not a valid parameter to use for a stability determination of three-lobed bearings that are not centrally lobed.

Lewis Research Center,
National Aeronautics and Space Administration,
Cleveland, Ohio, January 30, 1970,
129-03.

REFERENCES

1. Schuller, Fredrick T.; Anderson, William J.; and Nemeth, Zolton: Operation of Hydrodynamic Journal Bearings in Sodium at Temperatures to 800° F and Speeds to 12,000 rpm. NASA TN D-3928, 1967.

2. Schuller, Fredrick T.; Fleming, David P.; and Anderson, William J.: Experiments on the Stability of Water Lubricated Herringbone-Groove Journal Bearings. I-Theoretical Considerations and Clearance Effects. NASA TN D-4883, 1968.

3. Malanoski, S. B.: Experiments on an Ultrastable Gas Journal Bearing. J. Lubr. Tech., vol. 89, no. 4, Oct. 1967, pp. 433-438.

4. Vohr, J. H.; and Chow, C. Y.: Characteristics of Herringbone-Grooved, Gas-Lubricated Journal Bearings. J. Basic Eng., vol. 87, no. 3, Sept. 1965, pp. 568-578.

5. Lund, J. W.: Rotor-Bearing Dynamics Design Technology. Part 7: The Three Lobe Bearing and Floating Ring Bearing. Rep. MTI-67TR47, Mechanical Technology, Inc. (AFAPL-TR-65-45, pt. 7, DDC No. AD-829895), Feb. 1968.

6. Chadbourne, L. E.; Dobler, F. X.; and Rottler, A. D.: Snap 50/SPUR Nuclear Mechanical Power Unit Experimental Research and Development Program. Part 2: Bearings. Rep. APS-5249-R, Garrett Corp. (AFAPL-TR-67-34, pt. 2, DDC No. AD-815583), Dec. 31, 1966.

7. Schuller, Fredrick T.; Fleming, David P.; and Anderson, William J.: Experiments on the Stability of Water Lubricated Herringbone-Groove Journal Bearings. II-Effects of Configuration and Groove to Ridge Clearance Ratio. NASA TN D-5264, 1969.

NASA-Langley, 1970 — 15 E-5434

NATIONAL AERONAUTICS AND SPACE ADMINISTRATION
WASHINGTON, D. C. 20546

OFFICIAL BUSINESS

FIRST CLASS MAIL

POSTAGE AND FEES PAID
NATIONAL AERONAUTICS AND
SPACE ADMINISTRATION

POSTMASTER: If Undeliverable (Section 158 Postal Manual) Do Not Return

"The aeronautical and space activities of the United States shall be conducted so as to contribute . . . to the expansion of human knowledge of phenomena in the atmosphere and space. The Administration shall provide for the widest practicable and appropriate dissemination of information concerning its activities and the results thereof."

— NATIONAL AERONAUTICS AND SPACE ACT OF 1958

NASA SCIENTIFIC AND TECHNICAL PUBLICATIONS

TECHNICAL REPORTS: Scientific and technical information considered important, complete, and a lasting contribution to existing knowledge.

TECHNICAL NOTES: Information less broad in scope but nevertheless of importance as a contribution to existing knowledge.

TECHNICAL MEMORANDUMS: Information receiving limited distribution because of preliminary data, security classification, or other reasons.

CONTRACTOR REPORTS: Scientific and technical information generated under a NASA contract or grant and considered an important contribution to existing knowledge.

TECHNICAL TRANSLATIONS: Information published in a foreign language considered to merit NASA distribution in English.

SPECIAL PUBLICATIONS: Information derived from or of value to NASA activities. Publications include conference proceedings, monographs, data compilations, handbooks, sourcebooks, and special bibliographies.

TECHNOLOGY UTILIZATION PUBLICATIONS: Information on technology used by NASA that may be of particular interest in commercial and other non-aerospace applications. Publications include Tech Briefs, Technology Utilization Reports and Notes, and Technology Surveys.

Details on the availability of these publications may be obtained from:

SCIENTIFIC AND TECHNICAL INFORMATION DIVISION

NATIONAL AERONAUTICS AND SPACE ADMINISTRATION

Washington, D.C. 20546